International Journal of Technology 13(4) 870-879 (2022)
Received June 2021 / Revised April 2022 / Accepted June 2022

International Journal of Technology

http://ijtech.eng.ui.ac.id

Characterization and Potential Production of Glass-Ceramics Biomaterial from Basalt Rock of Local Lampung Province

Irza Sukmana[1*], Yusup Hendronursito[1,2], Shirley Savetlana[1], Kusno Isnugroho[2], Muhammad Amin[2], David Candra Birawidha[2]

[1]*Mechanical Engineering Department, Engineering Faculty, Universitas Lampung, Jl. Prof. Soemantri Brojonegoro No.1, Bandar Lampung 35143, Indonesia*
[2]*Mining Technology Research Center – National Research and Innovation Agency, Jl. Ir. Sutami Km. 15 Tanjung Bintang, Lampung Selatan 35361, Indonesia*

Abstract. Glass-ceramics were fine-grained polycrystalline materials produced by controlled crystallization in the glass phase to have outstanding characteristics. The establishment of basalt from Sukadana - Lampung Province into glass-ceramic begins with the process of reduced size and milled under 200 mesh using an ASTM sieve. The initiated glass-ceramics formation was created by melting the basalt powder at a temperature of 1,250°C for 2hrs to obtain the glass phase. Glass parent crystallization begins with the stage of nucleation growth. The nucleation process occurs at a temperature 600°C for 1hr. The crystallization temperature at variations of 850, 950, or 1,050°C for 3 and 8hrs. The mechanical hardness test result was 637.28 HV_{1N} of the sample with 1,050°C heating for 3hrs. The highest hardness value is at 837.33 HV_{1N} for a sample of 1,050°C heating for 8hrs. The hardness value was decreased at samples for 3hrs heating, while it increased for 8hrs of a heating process. All of the heating treatments formed olivine and Anorthite phase but a pyroxene phase was initiated from 950°C heating process for 3hrs. The use of glass ceramic as an engineering material and biomaterials are promising. It is necessary to continue the development studies on the production process of local basalt resources.

Keywords: Basalt; Crystallization; Glass ceramics; Hardness; Phase

1. Introduction

Glass-ceramics (G.C.s) were fine-grained polycrystalline materials produced by controlled crystallization in the glass phase (Rawlings et al., 2006). G.C.s are preferred for wear-resistant and corrosion-resistant electronics and medicine materials (Yilmaz et al., 2006). G.C.s can be produced by materials such as TiO_2-SiO_2 (Kusrini et al., 2017), SnO_2 and amorphous silica xerogel (S.X.) (Aripin et al., 2016) until waste-based materials (Rawlings et al., 2006).

G.C.s can be produced by sintered basalt. Basalt glass ceramics (BGCs) are used in many applications. For example, as a coating (Ateş et al., 2017; Yilmaz et al., 2006), bio-ceramics for an implant (SDVOSB, 2018), and for reinforcing material (Boshytska et al., 2017; Kaplunenko et al., 2016). The BGCs have a homogeneous structure of finely dispersed crystals (Yilmaz et al., 1996). Basaltic tuff was sintered at a temperature of 1,100°C showing

*Corresponding author's email: irza.sukmana@eng.unila.ac.id, Tel.: +62-721-704 947, Fax: +62-721-704 947
doi: 10.14716/ijtech.v13i4.4958

a similar structure to G.C.s and has characteristic 8-9% closed porosity and zero water absorption. The crystalline phase consisted of pyroxene, anorthite, spinel, and hematite. The BGCs with suitable properties such as a bending strength of 100 MPa and a elasticity modulus of 90 GPa (Karamanov et al., 2009). Compared with G.C.s from soda-lime-silica on the market, the BGCs are of great economic, technological, and scientific importance (Lopes & Shelby, 2005). BGCs have an extensive and low production cost with excellent mechanical, thermal, and chemical properties (Todic et al., 2011). The application of G.C.s in biomaterials can be divided into two groups: bone implant and dental restoration. G.C.s are a group of bioceramics potentially used for scaffolding (Habibie et al., 2019). Recent studies present the G.C.s in bone regeneration and tissue engineering (Lima et al., 2020).

Basalt is a volcanic igneous rock formed from the rapidly cooling of magma on the earth's surface. In the field of advanced materials, basalt can be used in the form of cast basalt (Isnugroho et al., 2020), fiber (Ivanitskii & Gorbachev, 2011), and composites (Subagia et al., 2017). In Indonesia, basalt is traditionally only used as a building material (Isnugroho et al., 2018). In less than the last five years, basalt in Indonesia has begun to be used as an advanced material, including as a substitute material for cement clinker (Amin et al., 2020), soil fertilizer (Hendronursito et al., 2019), PCC aggregate materials (Rajiman et al., 2018), and filler for paving block material (Muttaqii et al., 2020).

This study aims to determine the potential use of basalt rock from the Sukadana area in Lampung Province for G.C.s biomaterial application.

2. Methods

The basalt rock was obtained from Sukadana-East Lampung, Indonesia. Basalt crushed using jaw crusher and ball mill into powder size of under 200 mesh. The crystallization temperature is heated at three-time intervals for 3 or 8hrs holding time. Controlled crystallization of glass involves a two-stage the nucleation and crystallization stages. The thermal analysis's peak crystallization (Tx) and melting temperature (Tm) determine the glass-forming ability parameters. Based on recent thermal analysis, Tm and Tx divided into three levels (Matovic et al., 2003). The design of the experiment for each specimen is according to Table 1. The melting temperature was 1,250^{o}C for 1hr. The nucleation temperature was 600^{o}C for 2hrs. The heating rate of the muffle furnace was 10^{o}C/min.

Table 1 Parameter setting for specimen

No. Sample	R1	R2	R3	R4	R5	R6
Crystallization Temp. ^{o}C	850	950	1.050	850	950	1.050
Hold. Time	3hrs			8hrs		

Characteristics of BGCs were carried out by chemical composition analysis using XRF Epsilon 4 XRF Spectrometer from Malvern Panalytical, crystal phase formation using Panalytical Xpert 3 Powder XRD. Mechanical characteristics with micro Vickers hardness, density, and topography using SEM. The standard test method for micro indentation hardness of materials, according to ASTM E384 with 1N indentation load for 12 seconds, repeated six times for each specimen.

3. Results and Discussion

3.1. X-ray Fluorescence of Raw Basalt

The chemical concentration of raw basalt is shown in Table 2. The melting temperature, workability, and crystallization of glass depend on CaO/Na_2O and CaO/MgO ratio. CaO/MgO ratio has an essential role in promoting nucleation density. CaO to MgO and

CaO to Na_2O ratios are under 2.5 and 10, respectively. This intricate basalt-based glass is capable of crystallizing into a homogeneous and delicate structure.

Table 2 Dominant chemical composition of the raw basalt

Element	Concentration (%)
Na_2O	3.356
MgO	4.561
Al_2O_3	18.820
SiO_2	48.418
K_2O	0.636
CaO	9.761
TiO_2	1.329
Fe_2O_3	12.595

3.2. X-ray Fluorescence of BGCs

The results of the chemical analysis of BGCs are predominantly SiO_2, Fe_2O_3, Al_2O_3, CaO, ZnO, and MgO, as shown in Table 3.

Table 3 The chemical analysis of BGCs

Samples/ Contents	R1	R2	R3	R4	R5	R6
MgO	2.99	3.14	3.10	2.73	2.83	2.78
Al_2O_3	13.92	14.4	14.32	13.65	13.46	14.84
SiO_2	38.00	40.39	39.69	37.74	38.95	41.53
K_2O	0.62	0.68	0.66	0.65	0.68	0.86
CaO	11.79	12.83	12.06	11.41	12.26	11.86
TiO_2	1.82	2.01	1.94	1.81	1.94	1.91
Fe_2O_3	22.44	18.42	19.07	22.00	19.65	18.62
ZnO	4.90	5.29	5.85	6.31	6.71	4.33

The chemical percentage change is minimal compared with all specimen. The SiO_2 content is between 37.739 and 41.534%, which is an essential factor when melting and casting. The SiO_2 content below 50% indicates a lower melt viscosity value (Matovic et al., 2003). The decrease in viscosity value is also influenced by the high of Fe_2O_3, MgO, and CaO. The samples showed the content of glass-forming oxide (SiO_2+Al_2O_3), which will produce good chemical resistance from six different treatments. The alkali metal content (0.6%) is very small, so it does not significantly reduce the melting temperature. Likewise, the chemical content of TiO_2 can be neglected, but its existence is very important because of its mineralization. The high crystallization tendency is also indicated by the TiO_2 composition, which is in the range of 2% titanium (Ergul et al., 2007). Ti oxide causes the spontaneous formation of delicate crystal structures.

Figure 1 shows the temperature effect on changes in FeO. Fe_2O_3 was obtained from the X-ray fluorescence test, while FeO was calculated stoichiometrically. It had a negligible impact on the quantity of iron at higher temperatures. The crystallisation temperature at 950°C showed that the iron oxide content was the most minor compared to other temperatures for both 3 and 8hrs holding times. On containment, the crystallization rate shows the same decreasing trend from temperature 850, 950, and 1,050°C, which is 15wt%.

However, at 850 and 1,050°C, there was no significant difference in the effect of the crystallization treatment duration of 3 and 8hrs.

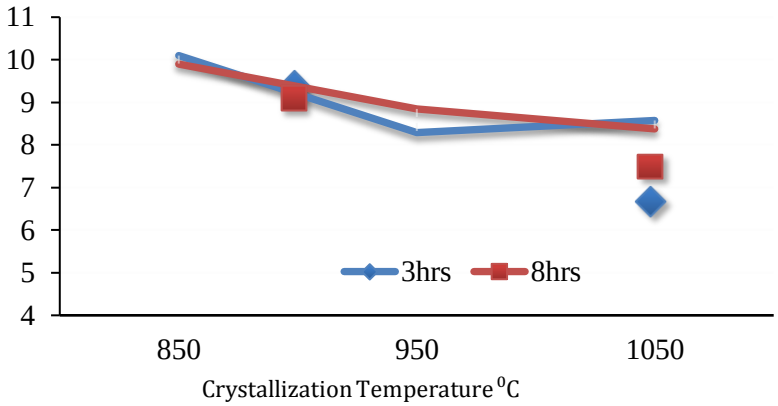

Figure 1 Effect of temperature on the oxidation state of the sintered bodies

The difference in temperature and crystallization time has no significant effect on producing the iron number (Fe^{3+}). The reduced FeO oxidation was affected by temperature and the crystallization elongation time. Ferric iron in G.C.s has an apparent effect on increasing uniform crystallization at relatively lower temperatures. The FeO/Fe_2O_3 ratio obtained in the experiments ranged from 0.76 to 0.72. A ratio higher than 0.5 is promote the nucleation process of Fe^{3+} into magnetite. When heat-treated at temperature between 650 – 800°C, the magnetite nuclei act as a nucleating agent (de Lima et al., 2021).

3.3. X-ray Diffraction of Raw Basalt

The result of X-Ray Diffraction of raw basalt content of anorthite, olivine, and pyroxene phase, is showed in Figure 2. The crystalline phases that formed in raw basalt are anorthite ($Ca_8Si_{16}Al_{16}O_{64}$), oliven ($Mg_{4.56}Fe_{3.3}Mn_{0.12}Ca_{0.02}Si_4O_{16}$), and pyroxene (MgFeSiO). An anorthite is a group of plagioclase rock-forming minerals. The dominant composition of olivine affects the melting point of these minerals. The XRF of BGCs shows that Fe is more prevalent than Mg, so that the olivine in G.C.s is a type of fayalite. Although olivine is generally green, due to its high content of Fe (fayalites), the melted G.C.s is brownish.

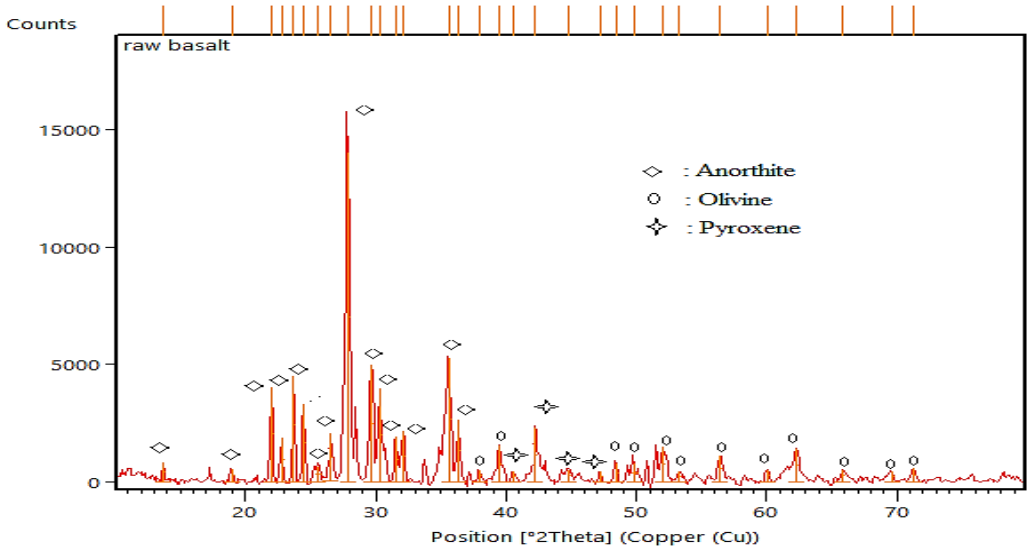

Figure 2 XRD of raw basalt from Sukadana area at Lampung Province

3.4. X-ray Diffraction of BGCs

Figure 3 shows the comparison of X-RD BGCs (R1-R6), showing the crystal peaks formed.

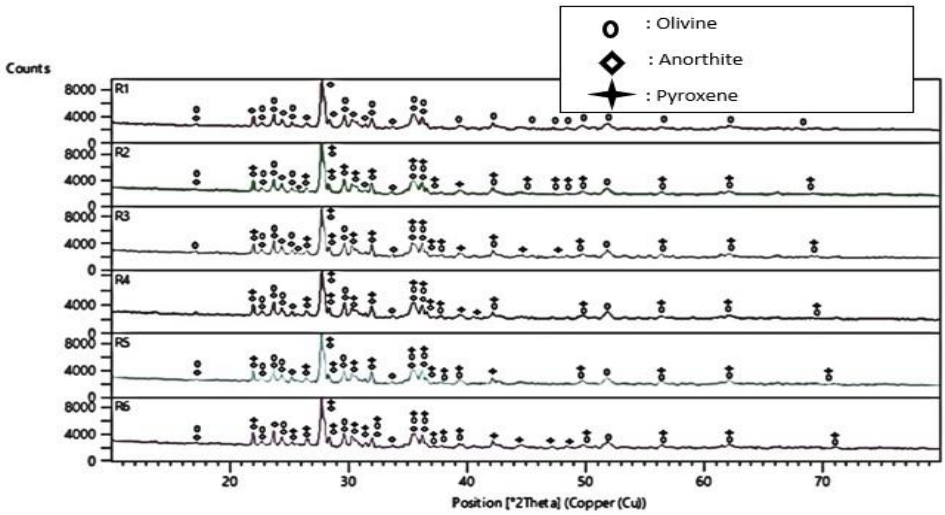

Figure 3 Comparison of BGCs XRD analysis

The result of XRD analysis for all samples shows anorthite ($Ca_8Si_{16}Al_{16}O_{64}$) and olivine ($Mg_{4.56}Fe_{3.3}Mn_{0.12}Ca_{0.02}Si_4O_{16}$). While in the samples R2 until R6 appearance of pyroxene crystal phase (MgFeSiO). These two crystalline phases are present in each sample. In the comparison chart R1 with other samples, there is no change in the intensity explicitly from the anorthite line. Anorthite is a group of plagioclase rock-forming minerals that are widespread in nature. The Anorthite structure is included in the group SiO_4 and AlO_4 tetrahedra connected by Ca^+. BGCs with an anorthite crystal phase can be used as a bioceramic material and are bio-acceptable because they are non-toxic and non-dangerous. The binary anorthite system holds promise as a biomedical material such as prostheses or tooth root material (Agathopoulos et al., 2003). G.C.s with the main crystal phase anorthite will have a low dielectric constant and a moderate coefficient of thermal expansion of the final product (Abdel-Hameed & Bakr, 2007). The low-moderate thermal expansion of G.C.s exerts an effect on crack resistance due to internal residual stress (Villas-Boas et al., 2020). Because of these properties, G.C.s based on anorthite are widely used in ceramics or porcelain in wireless communication devices and computers such as Low-Temperature Cofired Ceramic (LTCC) (Lo et al., 2002).

The olivine crystal phase was non-dominant in each sample. Olivine is a magnesium silicate mineral. The olivine in the BGCs is a form of fayalite since the BGCs demonstrate that Fe is more prominent than Mg. Although olivine is generally green in color, which is rich in Fe, it will produce a brownish color. The color of G.C.s tends to be brownish-black. Olivine also has heat resistance properties, so it is widely used as a refractory brick material (Geologinesia, 2016). The presence of olivine crystals affects the melting and cooling processes of BGCs. The olivine and pyroxene increased the mechanical and physical properties compared to raw basalt. G.C.s made from sintered basalt are more homogeneous structures with individual holes due to smaller cavitation (Pavlović et al., 2019).

3.5. Microhardness Analysis (H.V.)

The highest hardness was obtained from testing on sample R6 with an average hardness value of 837.33 HV. The graph shows a hardness changed in the holding time of 3 to 8hrs. The sintering process in 3hrs detention showed a decrease in the hardness value by 11.3%, while in sintering with 8hrs detention, there was an increase in the hardness

value by 31.39%. The holding time is an effort to control the nucleation process of crystal formation when sintering basalt in the form of glass. The length of detention and temperature significantly affect the crystal formation that occurs. The hardness of BGCs increased directly proportional to the crystallization temperature at a holding time of 8hrs. High temperature and sufficient holding time can provide perfect crystal formation time in basalt glass materials.

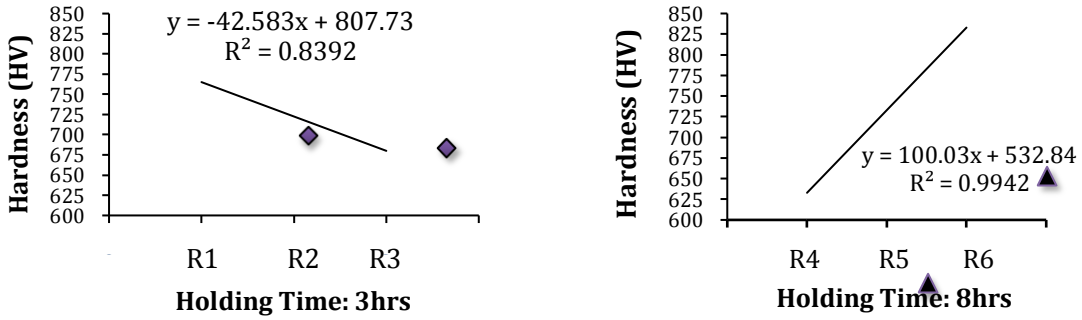

Figure 4 The hardness by the holding time: (a) 3hrs; and (b) 8hrs

According to the bioceramics hardness model study, there is a critical temperature point at which the relationship between temperature and hardness changes (Afriani and Tiandho, 2002). The selection of the right temperature and holding time will give the desired hardness.

3.6. Density analysis

The results of the basalt density are shown in Table 4 below. The density of BGCs is 1.9 to 2.9 g/cm^3. The treatment temperature affects the bulk density of BGCs. The crystallization formation process affects the crystallinity that forms in the G.C.s phase (Lima et al., 2020).

Table 4 The Result of the density test of BGCs

No. Sample	R1	R2	R3	R4	R5	R6
Crystal. Temp. (^{o}C)	850	950	1,050	850	950	1,050
Hold. Time (hrs)	3	3	3	8	8	8
Density (g/cm^3)	1.958	2.208	2.998	2.36	2.648	2.648

3.7. Microstructure Analysis

The microstructural images of BGCs heat product samples are shown in Figures 5. There are bubbles of various sizes at 850^{o}C for 3hs. These bubbles on the surface cause surface roughness. The process of sintering basalt into G.C.s causes the formation of shock energy. This shock energy gives the effect of the bubbles formed on the G.C.s surface (Pavlović et al., 2019). A white stripe pattern in 950^{o}C - 3hrs indicates the formation of G.C.s. As seen in a red circle in Figure 5 (c), the sample at 1,050^{o}C - 3hrs has some structurally fragile patches. A decrease in the hardness value was obtained in 1,050^{o}C - 3hrs. The surface morphology of the 850^{o}C - 8hrs also shows the presence of a brittle area as in 1,050^{o}C - 3hrs. The hardness of 1,050^{o}C - 3hrs and 850^{o}C - 8hrs were the samples with the lowest hardness values of 669.21 HV and 637.20 HV, respectively. The brittle surface structure causes the hardness of these two samples to be low compared to the other samples.

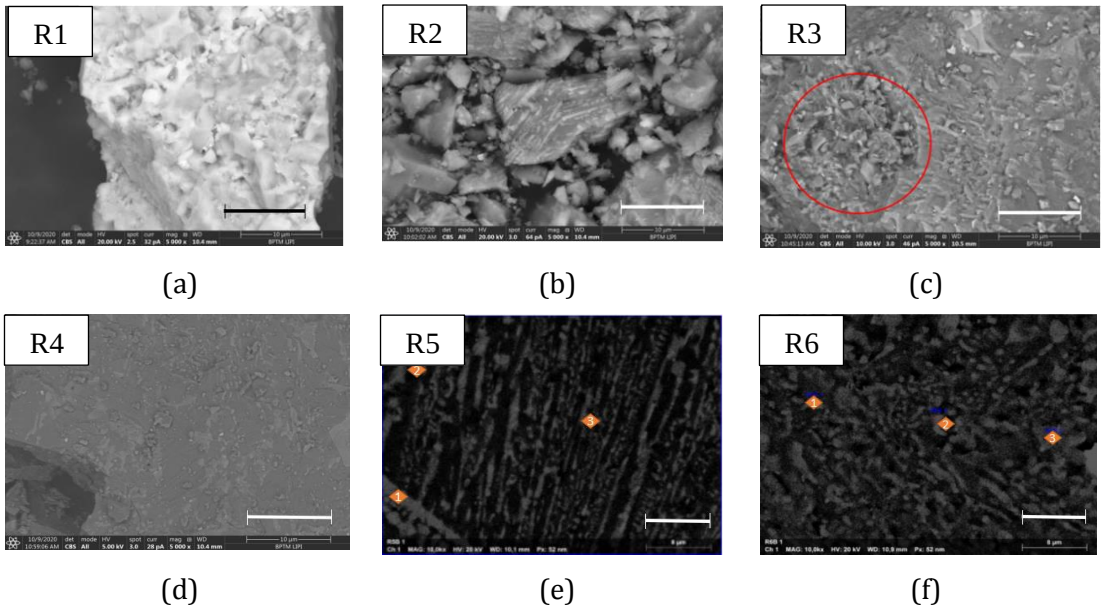

Figure 5 Scanning electron microscopy of G.C.s obtained at: (a) 850°C-3hrs; (b) 950°C-3hrs; (c) 1,050°C-3hrs; (d) 850°C-8hrs; (e) 950°C-8hrs; and (f) 1,050°C-8hrs. Bars were 10µm.

In 950°C - 8hrs, there is a white stripe patterns. These patterns indicate the pyroxene phase (MgFeSiO) when seen in Table 5 EDX spot 1 (white stripes): dominant Si, Fe, Mg. EDX spot 2 (black area): dominant Si, Al, Ca indicates anorthite crystal phase. EDX spot 3 (white, gray/ slightly dark color): dominant Si, Al, Mg, Fe, Ca indicating anorthite and olivine phases.

The patterns at 1,050°C - 8hrs that is formed is similar to those at 950°C - 8hrs. There are white stripe patterns, indicating the formation of a pyroxene phase more dominant than the previous process. In this sample, the highest hardness value is 837.33 HV. Sample 1,050°C - 8hrs was obtained from crystallization treatment at a temperature of 1,050°C, holding time 8 hrs.

Table 5 SEM - EDS test results for BGCs

Element	Spot 1 Mass (%)	Spot 2 Mass (%)	Spot 3 Mass (%)
Carbon	4.28	3.63	4.31
Oxygen	42.2	46.51	44.42
Sodium	2.71	3.85	2.94
Magnesium	7.32	1.93	5.08
Aluminum	6.28	10.41	9.04
Silicon	16.61	19.98	18.32
Calcium	4.3	7.65	5.15
Iron	11.41	3.44	7.11
Zinc	4.04	1.26	2.88

The chemical composition of BGCs binds to each other and forms a crystalline phase characterized by different colors. The dominance of the crystals formed affects the hardness of G.C.s.

4. Conclusions

The chemical and mineral composition of Sukadana - East Lampung basalt allows the formation of glass-ceramics at relatively low temperatures. The anorthite phase present in all samples. Basalt melts have the ability to produce glass-ceramics. The crystalline phase significantly influences the hardness of glass-ceramics. East Lampung basalt has a high iron oxide content which affects of the glass-ceramics hardness. Glass-ceramics with high iron oxides have a bubble structure in the form of glass. Besides being seen in the topography through the SEM test, low mechanical properties are also characterized by the presence of a more dominant olivine (fayalite) phase. The longer holding time provides sufficient time for the crystallization process to occur with the dominant pyroxene phase. This causes the formed glass-ceramics to have a high hardness with a finer structure. Glass-ceramics made from Sukadana Basalt have good properties and can be developed as bioceramics that require high hardness.

Acknowledgements

This research was supported in some parts by the BLU Universitas Lampung of "Penelitian Terapan" grant FY 2021 contract no. 1583/UN26.21/PN/2021. The authors acknowledge the facilities, scientific and technical support from Advanced Characterization Laboratories Lampung, National Research and Innovation Agency through E- Layanan Sains, Badan Riset dan Inovasi Nasional.

References

Abdel-Hameed, S.A., Bakr, I.M., 2007. Effect of Alumina on Ceramic Properties of Cordierite Glass–Ceramic from Basalt Rock. *Journal of the European Ceramic Society*, Volume 27(2-3), pp. 1893–1897

Afriani, F., Tiandho, Y., 2020. Development of Hydroxyapatite-Based Bioceramic Hardness Model Based on Variations in Synthesis Conditions. *Journal of Innovation and Technology*, Volume 1(1), pp. 33–38

Agathopoulos, S., Tulyaganov, D.U., Marques, P.A.A.P., Ferro, M.C., Fernandes, M.H.V., Correia, R.N., 2003. The Fluorapatite–Anorthite System in Biomedicine. *Biomaterials*, Volume 24(7), pp. 1317–1331

Amin, M., Birawidha, D.C., Muttaqii, M.A., Isnugroho, K., Hendronursito, Y., 2020. The Effect of Combustion Temperature on The Characteristic of Clinker. *In*: Proceedings of the 3rd International Seminar on Metallurgy and Materials 2019, Serpong 23-24 October, Indonesia

Aripin, H., Mitsudo, S., Sudiana, I.N., Priatna, E., Kikuchi, H., Sabchevski, S., 2016. Densification Behavior of SnO_2-glass Composites Developed from the Incorporation of Silica Xerogeland SnO_2. *International Journal of Technology,* volume 7(3), pp. 401–407

Ateş, A., Önen, U., Ercenk, E., Yılmaz, Ş., 2017. Crystallization Behaviors and Seal Application of Basalt Based Glass-ceramics. *In*: Proceedings of the 6th International Advances in Applied Physics and Materials Science Congress and Exhibition, Istanbul 1-3 June, Turkey

Boshytska, N.V, Fedorenko, Y.O., Perekos, A.O., Kaplunenko, N.V., 2017. Stability Of the Phase Composition of Hydroxyapatite Powder Systems Reinforced with Basalt Scale, When Interacting with Biological Environments. *Powder Metallurgy and Metal Ceramics*, Volume 55, pp. 574–579

De Lima, L. F., Perottoni, C. A., Zorzi, J. E., & Cruz, R. C. D., 2021. Effect of iron on the microstructure of basalt glass-ceramics obtained by the petrurgic method. *International Journal of Applied Ceramic Technology*, 18(6), 1950–1959. https://doi.org/10.1111/ijac.13865

Ergul, S., Akyildiz, M., Karamanov, A., 2007. Ceramic Material from Basaltic Tuffs. *Industrial Ceramics,* Volume 27(2), pp. 1–6

Geologinesia, 2016. Mineral Olivin: Pengertian, Genesa, Deskripsi dan Kegunaannya, Available Online at: https://www.geologinesia.com/2016/09/mineral-olivin-pengertian-genesa.html, Accessed on February 2, 2020

Habibie, S., Tristiyanti, Y., Gustiono, D., Harahap, M.E., Chalid, S.Y., Effendi, D., 2019. Production and Characterization of Scaffold made of Hydroxyapatite and Pectin of Green Cincau Leaf (Premna Oblongifolia Merr). *Journal of Engineering and Scientific Research,* Volume 1, pp. 12–17

Hendronursito, Y., Barus, J., Amin, M., Al Muttaqii, M., Rajagukguk, T.O., Isnugroho, K., Birawidha, D.C., 2019. The Local Mineral Potential from East Lampung-Indonesia: The Use of Basalt Rock as a Stone Meal for Cassava Plant. *Journal of Degraded and Mining Lands Management*, Volume 7(1), pp. 1977–1985

Isnugroho, K., Birawidha, D. C., Hendronursito, Y., Amin, M., Muttaqii, M. Al, Efriyo Hadi, R. A., & Fazma, M. F., 2020. Preliminary Study of Melting Basalt Rock As A Raw of Advanced Material. *In:* IOP Conference Series: Materials Science and Engineering, 807(1). https://doi.org/10.1088/1757-899X/807/1/012001

Isnugroho, K., Hendronursito, Y., Candra, B.D., 2018. Characterization and Utilization Potential of Basalt Rock from East- Lampung District. *In:* Proceeding of Mineral Processing and Technology International Conference, Jakarta 23-24 October, Indonesia

Ivanitskii, S.G., Gorbachev, G.F., 2011. Continuous Basalt Fibers: Production Aspects and Simulation of Forming Processes. I. State of the Art in Continuous Basalt Fiber Technologies. *Powder Metallurgy and Metal Ceramics*, Volume 50(3), pp. 125–129

Kaplunenko, N.V, Ulyanchych, N.V, Klipov, V.D., Gorban, V.F., 2016. Refractory And Ceramic Materials Basalt Scale-Reinforced Hydroxyapatite. *Powder Metallurgy and Metal Ceramics*, Volume 55, pp. 306–311

Karamanov, A., Arrizza, L., Ergul, S., 2009. Sintered Material from Alkaline Basaltic Tuffs. *Journal of The Europe Ceramic Society,* Volume 29(4), pp. 595–601

Kusrini, E., Kartohardjono, S., Sofyan, N., Yuwono, A.H., 2017. Innovation of Renewable Energy, CO2 Capture and Storage Materials for Better Applications. *International Journal of Technology*, volume 8(8), pp. 1371–1375

Lima, L.F., Mantas, P.Q., Segadães, A.M., Cruz, R.C., 2020. Processing and Characterization of Sinter-Crystallized Basalt Glass-Ceramics. *Journal of Non-Crystalline Solids,* Volume 538, pp. 1–7

Lo, C.L., Duh, J.G., Chiou, B.S., Lee, W.H., 2002. Low-Temperature Sintering and Microwave Dielectric Properties of Anorthite-Based Glass-Ceramics. *Journal of the American Ceramic Society,* Volume 85(9), pp. 2230–2235

Lopes, M., Shelby, J.E., 2005. *Introduction to Glass Science and Technology*. Royal Society of Chemistry., Cambridge, UK

Matovic, B., Boskovic, S., Logar, M., 2003. Preparation of Basalt-Based Glass Ceramics. *Journal of The Serbian Chemical Society,* Volume 68, pp. 505–510

Muttaqii, M.A., Amin, M., Handoko, A.S., Birawidha, D.C., Isnugroho, K., Hendronursito, Y., Rahayu, N., Syafriadi., 2020. The Characterization and Physical Properties of Paving Block Products Over Basalt Minerals. *In*: Proceedings of the 3rd International Seminar on Metallurgy and Materials 2019, Serpong 23-24 October, Indonesia

Pavlović, M., Dojčinović, M., Prokić-Cvetković, R., Andrić, L., 2019. The Mechanisms of Cavitation Erosion of Raw and Sintered Basalt. *Science of Sintering*, Volume 51(4), pp. 409–419

Rajiman, Alisjahbana, S.W., Riyanto, H., Hasyim, C., Setiawan, M.I., Harmanto, D., Wajdi, M.B.N., 2018. Substitution local resources basalt stone scoria Lampung, Indonesia, as a third raw material aggregate to increase the quality of portland composite cement (PCC). *International Journal of Engineering & Technology,* Volume 7(2), pp. 484–490

Rawlings, R.D., Wu, J.P., Boccaccini, A.R., 2006. Glass-Ceramics: Their Production From Wastes — A Review. *Journal of Materials Science*, Volume 41, pp. 733–761

SDVOSB., 2018. Trap Rock/Basalt Powder & Fiber. Reade Int. Corp, Available Online at: https://www.reade.com/products/trap-rock-basalt-powder-fiber, Accessed on November 3, 2020

Subagia, I.D.G.A., Sugita, I.K.G., Wirawan, I.K.G., Dwidiani, N.M., Yuwono, A.H., 2017. Thermal Conductivity of Carbon/Basal Fiber Reinforced Epoxy Hybrid Composites. *International Journal of Technology*, volume 8(8), pp. 1498–1506

Todic, A., Nedeljkovic, B., Cikara, D., Ristovic, I., 2011. Particulate Basalt–Polymer Composites Characteristics Investigation. *Materials & Design,* Volume 32(3), pp. 1677–1683

Villas-Boas, M. O. C., Serbena, F. C., Soares, V. O., Mathias, I., & Zanotto, E. D., 2020. Residual stress effect on the fracture toughness of lithium disilicate glass-ceramics. *Journal of the American Ceramic Society*, *103*(1), 465–479. https://doi.org/10.1111/jace.16664

Yilmaz, S., Bayrak, G., Sen, S. Sen, U., 2006. Structural Characterization of Basalt-Based Glass–Ceramic Coatings. *Materials and Design,* Volume 27, pp. 1092–1096

Yilmaz, S., Özkan, O.T., Günay, V., 1996. Crystallization Kinetics of Basalt Glass. *Ceramics International*, Volume 22(6), pp. 477–481